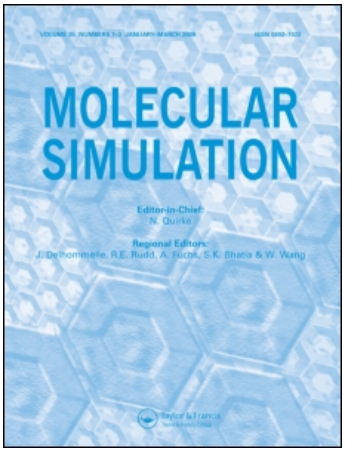

Molecular Simulation
Publication details, including instructions for authors and subscription information:
http://www.informaworld.com/smpp/title~content=t713644482

Structure of Lennard-Jones fluid near large spherical particles: further test of the "universality" of adjustable parameter in perturbation density functional theory

F. Luo[a]; A. Jamnik[b]; Y. Su[a]
[a] Institute of Modern Statistical Mechanics, Hunan University of Technology, Zhuzhou city, People's Republic of China [b] University of Ljubljana, Faculty of Chemistry and Chemical Technology, Ljubljana, Slovenia

To cite this Article Luo, F. , Jamnik, A. and Su, Y.(2006) 'Structure of Lennard-Jones fluid near large spherical particles: further test of the "universality" of adjustable parameter in perturbation density functional theory', Molecular Simulation, 32: 5, 391 — 399
To link to this Article: DOI: 10.1080/08927020600675715
URL: http://dx.doi.org/10.1080/08927020600675715

Molecular Simulation, Vol. 32, No. 5, 30 April 2006, 391–399

Taylor & Francis
Taylor & Francis Group

Structure of Lennard–Jones fluid near large spherical particles: further test of the "universality" of adjustable parameter in perturbation density functional theory

F. LUO†, A. JAMNIK‡* and Y. SU†

†Institute of Modern Statistical Mechanics, Hunan University of Technology, Wenhua Road, Zhuzhou city 412008, People's Republic of China
‡University of Ljubljana, Faculty of Chemistry and Chemical Technology, Aškerčeva 5, SI-1001 Ljubljana, Slovenia

(Received December 2005; in final form March 2006)

Grand canonical Monte Carlo simulation is used to study the density profiles of Lennard–Jones (LJ) fluid next to a large hard sphere (mimicking a colloidal particle) of various sizes. The LJ fluid in the inhomogeneous system thus maintains equilibrium with the bulk LJ fluid. The chosen density and potential parameters for the bulk fluid correspond to the conditions situated at "dangerous" regions of the phase diagram, i.e. near the critical temperature or close to the gas–liquid coexistence curve. The aim of present extensive simulations is to provide exact data for the broad range of the bulk parameters against which the "universality" of adjustable parameter associated with a perturbation density functional approximation (DFA) can be tested. Here the term "universality" means independence of this parameter on the particular external field responsible for the generation of a non-uniform density profile of the fluid. It is shown that the "universality" of this parameter associated with a third order + second order perturbation DFA holds also in the present case of a large spherical particle as a source of external potential, similarly as established in previous studies dealing with other interaction potential and other external fields [*J. Chem. Phys.*, **122**, 064503 (2005); *J. Chem. Phys.*, **123** 124708 (2005)]. This DFA can be used as input into a recently proposed framework for the calculation of interparticle potential of mean force (PMF).

Keywords: Simulation; Adsorption; Interface; DFA

1. Introduction

Theoretical study of the structural and related thermodynamic properties of asymmetric fluid mixtures is very important for understanding a variety of problems in colloid physics. Namely, a colloid dispersion can be modeled as a multicomponent system formed by large (macro) particles mimicking colloidal solute and smaller molecules denoting the solvent component. The determination of the local structure of such inhomogeneous systems has, therefore, long been the subject of intense theoretical research and numerous studies have reported the results of thermodynamic and structural properties of fluids in the vicinity of macroparticles of different shapes [1–5]. A particular attention has been paid to the dependence of these properties on the size of colloidal macroparticles. The structure of the molecular solvent in the interface among colloidal particles is also responsible for the intercolloidal solvation force, often called also as solvent mediated or structural force emphasizing the source of its appearance. As colloidal particles take part in various chemical and biological reactions, knowledge of the solvation force is also of great practical importance. The simplest analytically tractable model, which combines both the hard-core repulsion and the short-ranged attraction, is Baxter's sticky hard sphere fluid (SHS) [6]. As an improved model to that considering the purely hard-core interactions among the solvent molecules, it has been used in providing the insights into solvation in colloidal [7–10] and confined systems [11–13]. Among more practical potentials, the Lennard–Jones (LJ) fluid has been the most frequently applied to model the attractive dispersion forces in a variety of physical situations ranging from the simplest case of modeling the interactions in simple fluids to much more complex systems including

*Corresponding author. Email: andrej.jamnik@fkkt.uni-lj.si

Molecular Simulation
ISSN 0892-7022 print/ISSN 1029-0435 online © 2006 Taylor & Francis
http://www.tandf.co.uk/journals
DOI: 10.1080/08927020600675715

solvent averaged interactions in colloidal suspensions. This model has been especially popular also as the sample model used for critical tests of statistical mechanical theories.

In our previous papers [14,15], LJ model was used to estimate the accuracy of the third order + second order perturbation density functional approximation (DFA) in predicting the structure of this fluid subjected to diverse external fields stemming from the presence of various spatial constrains reflecting various degree of confinement. For the latter, we have chosen in turn: a hard flat interface, a planar slit consisting of two parallel, perfectly smooth hard walls, and a closed spherical surface mimicking a spherical cavity. DFA predictions were tested against the results of a grand canonical ensemble Monte Carlo (GCEMC) simulation. In the present work, we report on an analogous study of the structure of LJ fluid around a large hard sphere of different size mimicking an inhomogeneous system formed by single spherical colloidal particle immersed in a LJ solvent. The motivation of the present investigation is to test and confirm the "universality" of an adjustable parameter associated with the third order + second order perturbation DFA [14,15] by comparison of the theoretical predictions with the extensive simulation results for dangerous regions in the phase diagram of the bulk fluid. However, these results will also serve as a useful starting point for the further investigation of solvent-induced excess potential of mean force (PMF) in the similar systems. In a recently proposed framework for the calculation of the solvent-induced excess PMF [16–19], the density profile of solvent particles around a single spherical solute particle is important input information. For this reason, a theoretical method yielding sufficient and reliable results for this inhomogeneous fluid structure is significant for numerical implementation of the calculation framework.

In regard to the theoretical calculation of the density profile of solvent particles near a single body, a powerful theoretical tool is the classical density functional theory (DFT) [20]. Since its introduction in classical statistical mechanics in 1979, the classical DFT has witnessed a great progress and until now the DFT has evolved into a most convenient and accurate tool for the study of various phenomena in inhomogeneous systems [21]. Considering the fact that the main purpose of the present paper is to test the "universality" of the adjustable parameter associated with the perturbation DFT, it is necessary to give in this introduction a concise chronological review about the development of DFT approximation, especially the series of contributions due to Zhou on which the present theoretical calculation is based on.

A starting point of classical DFT's development and application in liquid physics is the pioneering work on liquid–solid freezing transition by Ramakrishnan and Yussouff [22,23]. However, because of the second order truncation of the excess Helmholtz free energy, Ramakrishnan and Yussouff's approximation is quantitatively inaccurate. Then, based on intuitive consideration, third order functional perturbation expansion approximation (FPEA) was proposed, which employed a simple symmetric function [22,23]

$$C_0^{(3)}(\mathbf{r}_1,\mathbf{r}_2,\mathbf{r}_3) = B\int \mathrm{d}\mathbf{r}_4 a(\mathbf{r}_4-\mathbf{r}_1)a(\mathbf{r}_4-\mathbf{r}_2) \quad (1)$$
$$a(\mathbf{r}_4-\mathbf{r}_3)$$

The kernel functions in the above expression for the uniform third order direct correlation function (DCF) reads: $a(r) = \frac{6}{\pi\sigma^3}\Theta\left(\frac{\sigma}{2}-r\right)$, where Θ is the Heaviside unit-step function and σ the diameter of the particles. Due to an arbitrary choice of the kernel function, such third order FPEA is still unsuitable for its application in a quantitative sense. An important development of the FPEA in this direction is the high order DCF for the uniform fluid proposed by Zhou and Ruckenstein [24] based on a simple weighted density approximation (SWDA) [25]. The third order version of the high order DCFs is similar to that given by equation (1) but with an important difference that the kernel function is connected to the uniform second order DCF. In this approximation, of course, the kernel function is no more arbitrary. Subsequent development of third order perturbation DFA based on the third order DCF proposed in Ref. [24] indicated that the resultant third order perturbation DFA was excellent also quantitatively [26,27]. Especially in our recent investigations [14,15], based on global and new simulation results, we found that a combination of the third order DCF based on the SWDA and partitioned DFA [28–30] for the tail part of the interaction potential performs successfully only on condition of high accuracy of the input uniform second order DCF. Its accuracy and therefore applicability was found for both the supercritical and subcritical temperatures. For the hard sphere DFA, another significant development represents the weighted density approximation (WDA), which includes several different versions, i.e. the Tarazona's version [31], Ashcroft's version [32], and Rosenfeld's fundamental measure version [33]. However, computationally the simplest and quantitatively the most accurate is the bridge density functional approximation (BDFA) of Zhou and Ruckenstein [34,35]. Further development of the BDFA has proven that this theory could be extended to polymer melts [36], non-hard sphere fluids [37–39], especially the penetrable sphere fluid [40], and binary hard sphere mixtures [41,42] under the influence of external potentials. Zhou proposed also the numerical version of the BDFA [43,44]. In addition, the same author made another important development of the perturbation DFA referring to the so-called Lagrangian theorem-based density functional approximation (LTDFA) [45–50], which was extended also to binary hard sphere mixtures [51] and polymer melts [52]. Furthermore, based on the functional integration, Zhou extended the hard sphere

DFAs on the level of non-uniform first order DCF to calculate the non-uniform excess Helmholtz free energy and surface tension [53,54]. Besides the hard sphere DFAs based on the excess Helmholtz free energy and first order DCF, Zhou proposed also the hard sphere DFAs based on the bulk fluid radial distribution function (RDF) [55,56]. However, in contrast to the fast and extensive development of the hard sphere DFAs, the DFA for non-hard sphere fluids lag considerably behind. Nevertheless, there exist several routes that make possible the application of the hard sphere DFAs to study non-hard sphere fluids. First possibilities represent the density functional mean field approximation (DFMFA) and density functional perturbation approximation (DFPA) [57]; further chance refers to the partitioned DFA [28–30,58–60]. Besides these standard methodologies, there exists also a DFA based on the RDF denoted by RDF-based DFA [61,62]. Finally, some researchers employ the hard sphere DFAs directly to non-hard sphere fluids by substitution of the expressions for the hard sphere second order DCF and excess Helmholtz free energy appearing in the hard sphere DFAs by those corresponding to the non-hard sphere fluids [63–65]. Regarding the accuracy and related applicability of these methods, one can conclude that the DFMFA is very poor in this respect. The DFPA, on the other hand, makes somewhat better job in some cases but it becomes unsatisfactory at the low bulk densities and low temperatures. Incorporating an adjustable parameter [54], the accuracy of the one of the versions of the partitioned DFA [28–30] may be significantly improved. However, the corresponding formalism may not work for the subcritical temperatures. The reason for this deficiency is the fact that this formalism, as an input, needs the bulk second order DCF for many state points with the same temperature but different bulk densities that sometimes enter into the unstable region bounded by the binodal line. For these conditions, where the phase separation into dilute vapor and dense liquid phases occurs, the Ornstein–Zernike (OZ) integral equation has no physical solution. Although the RDF-based DFA may be very accurate and applied to subcritical temperatures, the many-value character originating from the bulk RDF hampers its development. Regarding the possibility for the direct application of the hard sphere WDAs to non-hard sphere fluids, the resultant formalism breaks down due to the same reason as explained in Refs. [28–30]. The DFAs that combine the convenience of high accuracy and their applicability to both supercritical and subcritical temperatures are the third order + second order perturbation DFA and a recently proposed universal theoretical way by Zhou [66,67,68].

The structure of the paper is organized as follows. The section 2 contains a brief description of the model and the methods used in this study, i.e. the GCEMC simulation and the third order + second order perturbation DFT approach. Numerical results for the density profiles are presented in the section 3, where the "universality" of the adjustable parameter in the perturbation DFT approach is tested. Finally, some concluding remarks are given in the last section 4.

2. Model and methods

2.1 The model

As in our previous work [15] we consider the LJ fluid with the potential function:

$$u_{lj}(r) = 4\varepsilon\left[\left(\frac{r}{\sigma}\right)^{-12} - \left(\frac{r}{\sigma}\right)^{-6}\right] \tag{2}$$

where ε and σ are the energy and size parameters of the potential, respectively. In the following the reduced units are used for the absolute temperature T, $T^* = kT/\varepsilon$ with k being the Boltzmann constant.

Further, the interaction among the LJ particles and large spherical particle of effective radius R is a hard core one:

$$\begin{aligned} \varphi_{\text{ext}}(\mathbf{r}) &= \infty \quad |\mathbf{r}| < R \\ &= 0, \quad \text{elsewhere} \end{aligned} \tag{3}$$

where φ_{ext} denotes the external potential.

2.2 Open ensemble simulation

For the LJ model of equation (2) we have carried out GCEMC simulations at constant chemical potential μ, volume V, and temperature T. This set of independent parameters that define the thermodynamic state of the system made possible the study of equilibrium between the bulk LJ fluid and the same fluid subjected to external field originating from the presence of the large spherical particle. The general features of the GCEMC method are described elsewhere [69]. Further, some details peculiar to this study are discussed in our previous works [14,15]. Therein, the results of independent simulations of the bulk LJ fluid are also presented. Apart from our interest in the bulk interparticle correlations, these simulations were needed to adjust the values of the chemical potential to the desirable bulk densities. Because of the equilibrium, of course, the same values for the chemical potential were then used in the simulation of the present inhomogeneous system, where, similarly as in the case of homogeneous (bulk) phase, the Monte Carlo (MC) cell was a cubic box with the periodic boundary conditions imposed in all three directions. The LJ fluid surrounded a large hard sphere located at the center of the cell. Simulations of the system with bigger central particle requested larger dimensions of MC box to assure distances larger than the distance where correlations between the hard particle from the basic MC cell and its images from the surrounding cells were still detected. In addition, our recent works mentioned above contain also the simulation results for the density profiles of the LJ fluid near a single hard wall. By considering the contact theorem, the value for an adjustable parameter was

determined from the corresponding simulation data for each set of the bulk potential and density parameters. This parameter is included in the DFA theory, which is briefly described in the next section.

The liquid–gas phase behavior of the pure LJ fluid was investigated by Potoff and Panagiotopoulos [70]. Using grand canonical MC simulations they determined the liquid–vapor coexistence curve and critical point. The critical parameters of the untruncated LJ potential were assessed as $T_c^* = 1.312$ and $\rho_c^* = 0.316$.

2.3 Third order + second order perturbation density functional theory

This paper represents a continuation of our previous DFA study of the structure of inhomogeneous LJ fluid [15]. Therefore, the reader is kindly advised to check the Section III of the Ref. [15] containing a detailed description of the third order + second order perturbation density functional theory and referred to some other papers dealing with DFA theory [24,28–30]. Here we show only the final result for the non-uniform DCF following from the DFA analysis [14,15]:

$$\begin{aligned} C^{(1)}(\mathbf{r};[\rho]\ldots) = C_0^{(1)}(\rho_b\ldots) &+ \int d\mathbf{r}'[\rho(\mathbf{r}') - \rho_b] \\ &\times C_0^{(2)}(|\mathbf{r}-\mathbf{r}'|;\rho_b\ldots) \\ &+ \lambda(\rho_b\ldots)\int C_{0\mathrm{hc}}^{(2)}(\mathbf{r},\mathbf{r}'';\rho_b\ldots) \\ &\left[\int C_{0\mathrm{hc}}^{(2)}(\mathbf{r}',\mathbf{r}'';\rho_b\ldots)(\rho(\mathbf{r}')-\rho_b)d\mathbf{r}'\right]^2 d\mathbf{r}'' \end{aligned} \tag{4}$$

where λ is an adjustable parameter and ρ_b the equilibrium bulk density. $C^{(n)}$ represents the non-uniform n-order DCF whereas $C_0^{(n)}$ refers to the corresponding uniform counterpart. The bulk second order DCF $C_0^{(2)}(r;\rho_b\ldots)$ is split into the hard-core part $C_{0\mathrm{hc}}^{(2)}(r;\rho_b\ldots)$ and tail part $C_{0\mathrm{tail}}^{(2)}(r;\rho_b\ldots)$. It is obtained numerically from the OZ integral equation combined by a suitable closure relation and an expression for the bridge functional [15,71,72]. Combination of equation (4) and the expression for the single component density profile given by:

$$\rho(\mathbf{r}) = \rho_b \exp\left\{-\beta\varphi_{\mathrm{ext}}(\mathbf{r}) + C^{(1)}(\mathbf{r};[\rho]\ldots) - C_0^{(1)}(\rho_b\ldots)\right\} \tag{5}$$

can be used to predict the density profile of the single component atomic fluid subjected to diverse external fields. Here, $\varphi_{\mathrm{ext}}(\mathbf{r})$ is the external potential responsible for the generation of the inhomogeneous spatial density distribution $\rho(\mathbf{r})$. In the present work the above equations (4) and (5) are applied for the calculation of the density profiles of LJ fluid under the influence of external potential denoted by equation (3).

First, the adjustable parameter λ for each set of parameters of the coexistence bulk fluid is determined by the single hard wall sum rule. The pressure of the equilibrium bulk fluid required for this purpose is obtained by considering the contact theorem relating the pressure and the single hard wall contact density. For the latter we employ the exact simulation result, the pressure being equal to $\rho(0.5\sigma)/\beta$. It means that the parameter λ is adjusted to the value ensuring the equality of the single hard wall contact density predicted by the present DFT approach and that obtained by "exact" simulation method. Because of the "universality" of the adjustable parameter λ one can use the same numerical value obtained from the single hard wall case also for other external potentials, here the one originating from the presence of a single large hard sphere, equation (3).

3. Numerical results and discussion

In figures 1–9, the GCEMC and density functional theory (DFT) results for the density profiles of the LJ fluid near large hard spheres in equilibrium with the bulk fluid are compared. The corresponding values for the adjustable parameter λ, obtained for each temperature and bulk density, are also presented. Calculations were performed for three reduced temperatures: at supercritical temperature $1.008{\cdot}T_c^*$, and at two subcritical temperatures $0.65{\cdot}T_c^*$ and $0.80{\cdot}T_c^*$, respectively. For the supercritical regime, the values of the bulk reduced density cover a broad range from 0.1 to 0.8. Subcritical regime, however, is represented by only a few values of the bulk density lying in narrow 1-phase regions of the phase diagram corresponding either to monophasic gaseous state (low densities) or monophasic liquid state (high densities). Three different sizes of the hard sphere are considered: the largest one with the radius $R' = 5\sigma$, a relatively small sphere of $R' = 1\sigma$, and one of intermediate size $R' = 2\sigma$. The centers of the particles of LJ fluid are, therefore, constrained to the distances $r > R = (R' + \sigma/2)$. Three

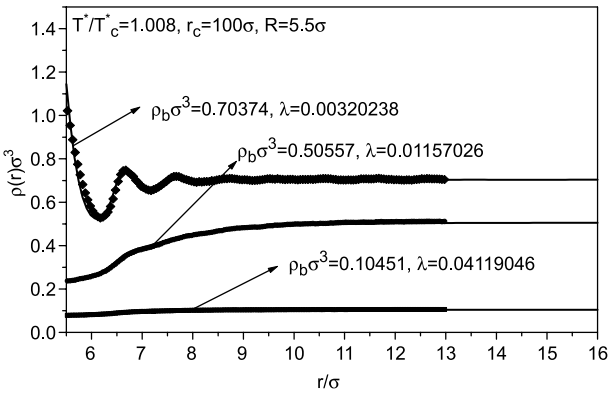

Figure 1. Monte Carlo (symbols) and density functional (lines) results for the density profiles of the LJ fluid near a large spherical particle of effective radius $R = 5.5\sigma$ at the supercritical reduced temperature $T^*/T_c^* = 1.008$ and at different values of the bulk reduced density. λ is the adjustable parameter determined by the single hard wall sum rule considering the contact theorem using the exact simulation results for the contact densities.

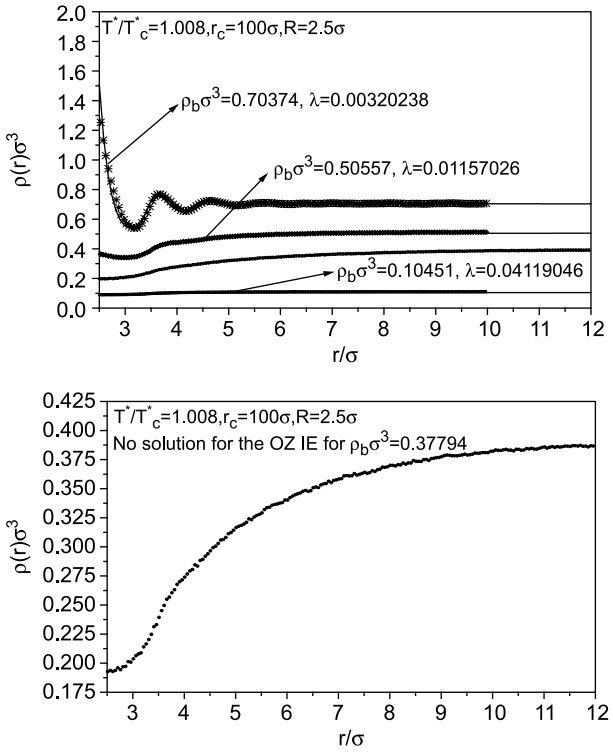

Figure 2. Same as figure 1 but for $R = 2.5\sigma$.

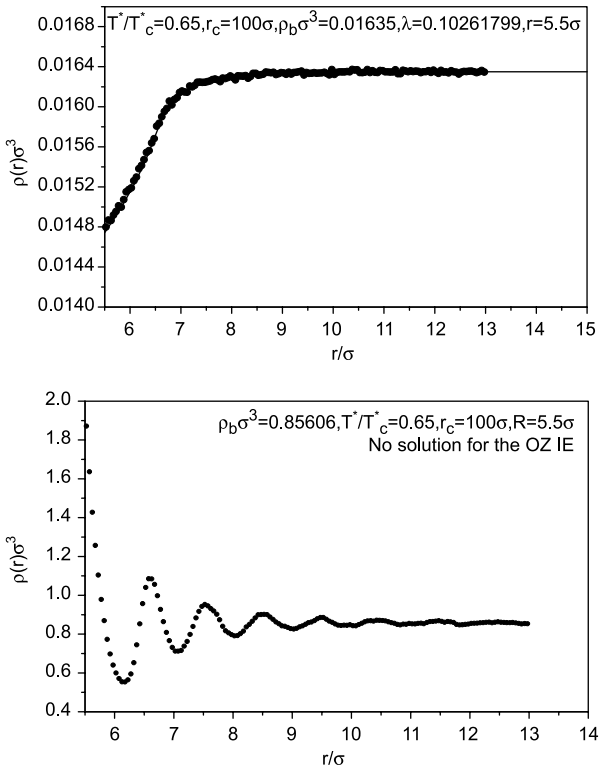

figure 4. Monte Carlo (symbols) and density functional (lines) results for the density profiles of the LJ fluid near a large spherical particle of effective radius $R = 5.5\sigma$ at the subcritical reduced temperature $T^*/T_c^* = 0.65$ and at two values of the bulk reduced densities: (i) $\rho_b\sigma^3 = 0.01635$ (gaseous state) and (ii) $\rho_b\sigma^3 = 0.85606$ (liquid state). λ is the adjustable parameter determined by the single hard wall sum rule considering the contact theorem using the exact simulation results for the contact densities.

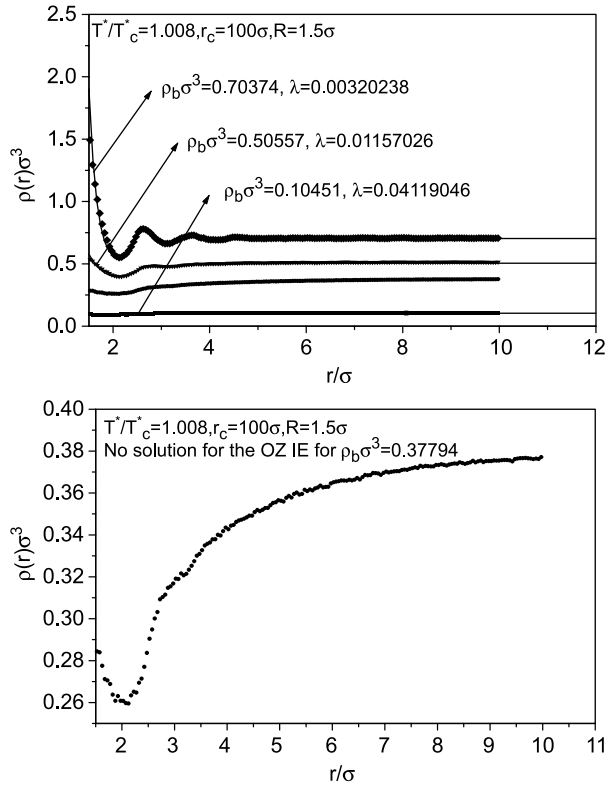

Figure 3. Same as figure 1 but for $R = 1.5\sigma$.

sets, each containing three figures (figures 1–9), refer to the three temperatures considered. Within the particular sets, the individual figures successively illustrate the effect of the decreasing of the size of the large sphere. For the sake of clarity, the majority of figures are subdivided into two or three parts, where the separate parts contain the results for the same set of the model parameters except the bulk densities.

A careful inspection of the presented local structures around the hard spherical body leads to a conclusion that the DFT predictions excellently agree with the simulation results. Except at the large sphere/fluid contact surface and its immediate vicinity, the DFT density profiles agree quantitatively with the simulation data. Both methods predict distinct density oscillations in the domain close to the surface of the large particle revealing important packing effects due to the finite size (excluded volume) of the molecules of the fluid. Of course, the amplitude of the oscillations depends on the density of the equilibrium bulk fluid and also on the temperature of the system. At higher temperatures, the attraction among the molecules loses in importance in comparison with their thermal energy. Such molecules thus resemble the hard (repulsive) particles that, due to the steric shielding effects, tend to accumulate adjacent to the boundary of the constraint thus giving rise to higher contact values and more pronounced oscillations

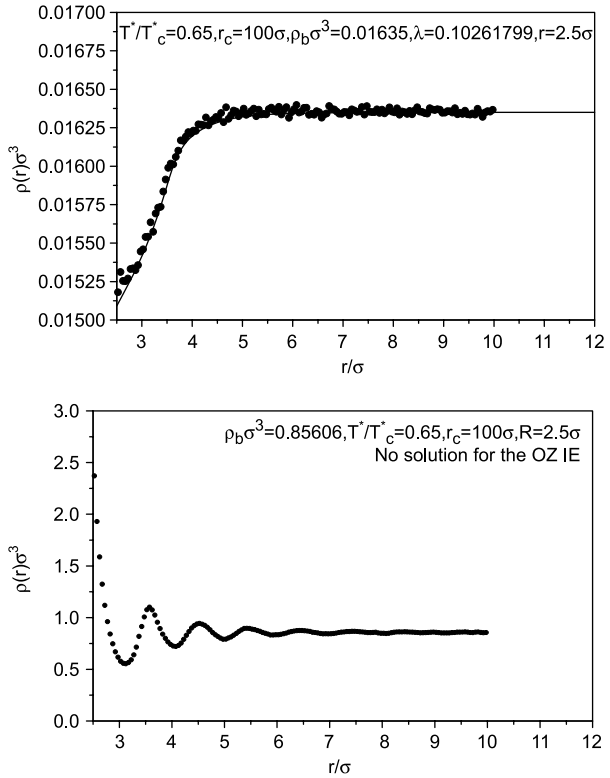

Figure 5. Same as figure 4 but for $R = 2.5\sigma$.

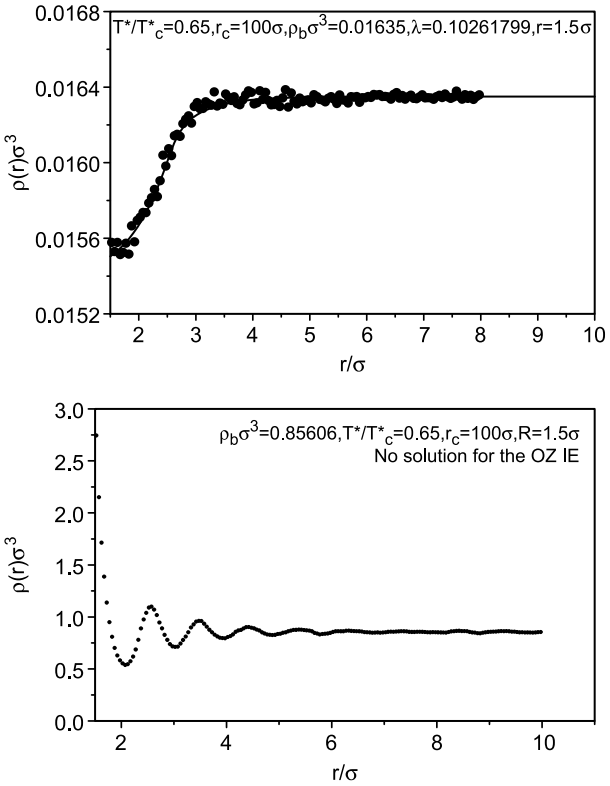

Figure 6. Same as figure 4 but for $R = 1.5\sigma$.

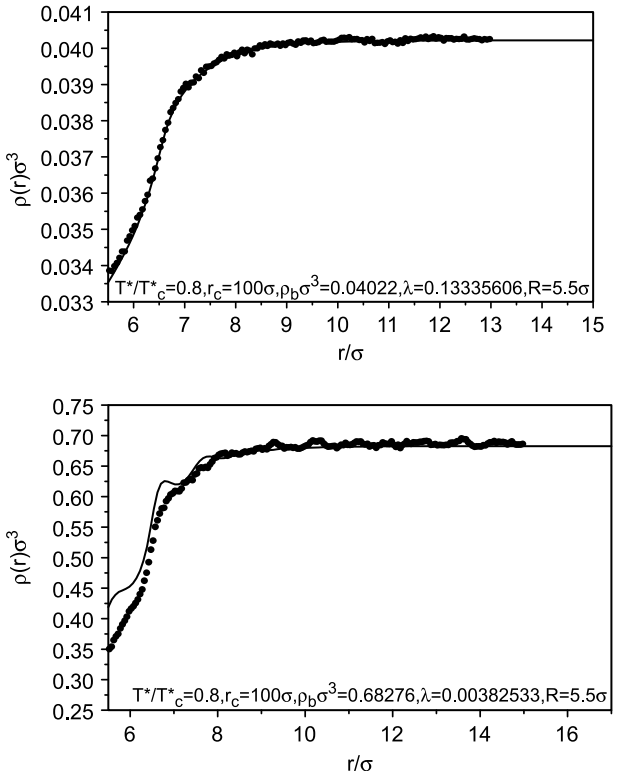

Figure 7. Monte Carlo (symbols) and density functional (lines) results for the density profiles of the LJ fluid near a large spherical particle of effective radius $R = 5.5\sigma$ at the subcritical reduced temperature $T*/T_c^* = 0.8$ and at two values of the bulk reduced densities: (i) $\rho_b\sigma^3 = 0.04022$ (gaseous state) and (ii) $\rho_b\sigma^3 = 0.68276$ (liquid state). λ is the adjustable parameter determined by the single hard wall sum rule considering the contact theorem using the exact simulation results for the contact densities.

of the density. Upon reducing temperature, the role of the attractive part in the intermolecular potential of interaction increases causing an efficient competition of interparticle attraction with the steric effects. In this case, the strongly attractive molecules try to avoid the region near the hard sphere as they have a better chance for mutual attraction at sufficient distances from the repulsive constraint. This leads to a reduction of the contact density and amplitude of the oscillations that gradually disappear. As noted above, the agreement between the theory and simulation is excellent except in close vicinity of the hard sphere/fluid contact plane where a slight deviation can be observed. This deviation slightly increases upon the reducing the size of large sphere. This is not surprising as the performance of the theory should improve with increasing the size of the macroparticles. Finally, it does the best job in the limit of infinite macroparticle size resembling a flat single hard wall.

A general observation following from the comparison between the theoretical DFT predictions and simulation data confirm the "universality" of the adjustable parameter λ, which is comprised in the DFT calculations. This means that it is independent on the external field responsible for the generation of the spatial inhomogeneous structure of the fluid. At a given set of bulk density and potential parameters, the value of this parameter is determined by

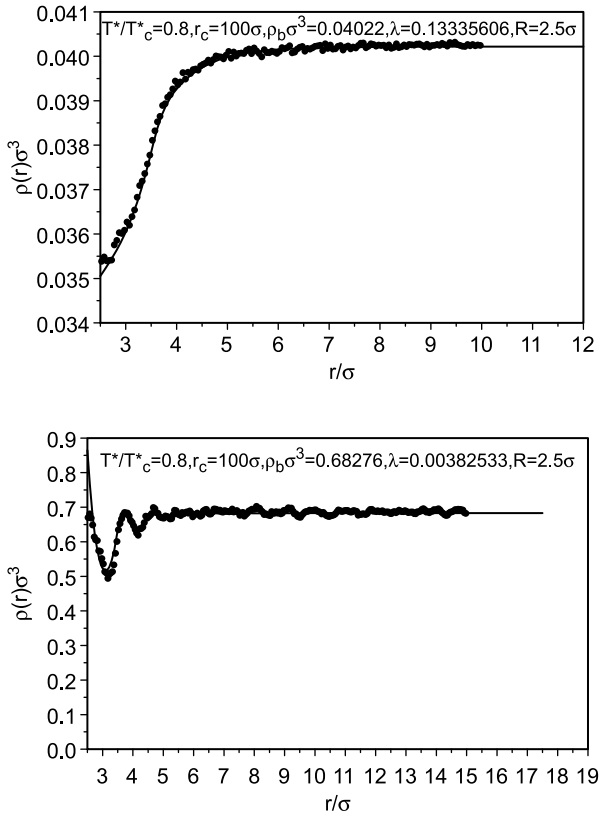

Figure 8. Same as figure 7 but for $R = 2.5\sigma$.

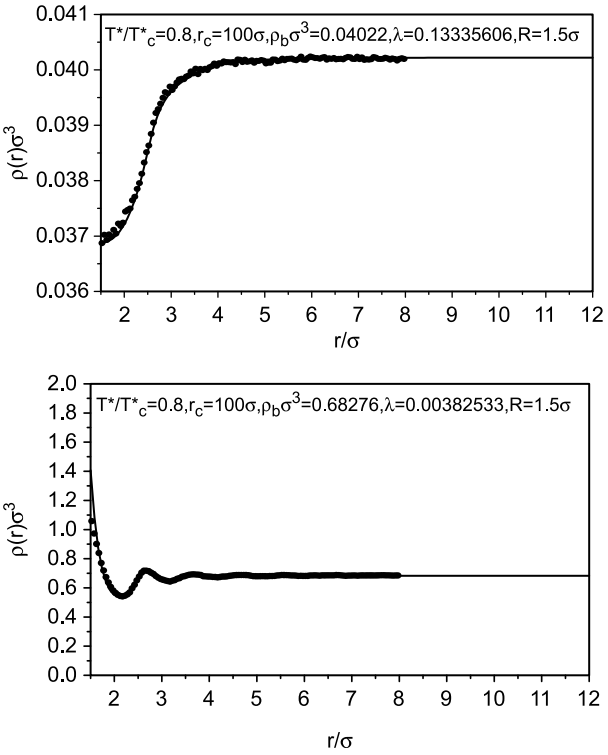

Figure 9. Same as figure 7 but for $R = 1.5\sigma$.

a single hard wall sum rule. The same value for λ can then be used in the case of other external potentials. An absence of the DFT results for the two sets of parameter: (i) $\rho_b\sigma^3 = 0.37794$, $T^*/T_c^* = 1.008$ (in the phase diagram, this supercritical state is located close to the critical point), and (ii) $\rho_b\sigma^3 = 0.85606$, $T^*/T_c^* = 0.65$ (this subcritical state is located in the vicinity of the gas–liquid coexistence curve), stem from the fact that there is no numerical solution to the Ornstein–Zernike (OZ) equation for these "severe" conditions. As discussed in our previous works, this deficiency of the theory is caused by the approximation made in the bridge function entering the OZ integral equation through a closure relation for the total correlation function and thus does not disprove the "universality" of the adjustable parameter.

4. Conclusions

In this paper we report extensive grand canonical Monte Carlo simulation study of the structure of LJ fluid near a single large hard sphere of various sizes. The LJ fluid in this inhomogeneous system maintains equilibrium with the bulk LJ fluid, which is at the conditions situated at "dangerous" regions of the phase diagram, i.e. the supercritical regions but near the critical temperature, or subcritical regions but close to the gas–liquid coexistence curve. The proposed simulation data for the broad range of model parameters serve as a strict standard test for the validity of any DFA, and concomitantly for the "universality" of the adjustable parameter, which is comprised in the DFA calculations. In this way, we found that the "universality" of this parameter holds also for the present inhomogeneous case. These results will also serve as a useful starting point for the further investigation of solvent-induced excess PMF in the similar systems. In a recently proposed framework [16–19] for the calculation of the solvent-induced excess PMF, the density profile of solvent particles around a single spherical solute particle is important input information. For this reason, a theoretical method yielding sufficient and reliable results for this inhomogeneous fluid structure is significant for numerical implementation of the calculation framework.

Acknowledgements

Support from the Slovenian Research Agency through the grants Nos. P1-0201 and J1-6653 is appreciated. This project is supported by the National Natural Science Foundation of China (Grant No. 20546004).

References

[1] G.I. Guerrero-Garcia, E. Gonzalez-Tovar, M. Lozada-Cassou, F.D. Guevara-Rodriguez. The electrical double layer for a fully

asymmetric electrolyte around a spherical colloid: an integral equation study. *J. Chem. Phys.*, **123**, 034703 (2005).
[2] H. Ohshima. Potential distribution around a charged spherical colloidal particle in a medium containing its counterions and a small amount of added salts. *Colloid Polym. Sci.*, **282**, 1185 (2004).
[3] D. Henderson, S. Sokolowski, A. Patrykiejew. Adsorption of fluids on colloidal particles—a density-functional approach. *Mol. Phys.*, **85**, 745 (1995).
[4] D. Henderson, C. Kwong-Yu, L. Degreve. The direct correlation-functions and bridge functions for hard-spheres near a large hard-sphere. *J. Chem. Phys.*, **101**, 6975 (1994).
[5] L. Degreve, D. Henderson. Monte Carlo study of the adsorption layers of hard-spheres near large large spheres of varying radii. *J. Chem. Phys.*, **100**, 1606 (1994).
[6] R.J. Baxter. Percus–Yevick equation for hard spheres with surface adhesion. *J. Chem. Phys.*, **49**, 2770 (1968).
[7] A. Jamnik, D. Bratko, D. Henderson. Liophobic interaction in Baxter adhesive fluid. *J. Chem. Phys.*, **94**, 8210 (1991).
[8] M.H.G. Penders, A. Vrij. Solvation interactions in colloidal dispersions using the adhesive hard-sphere model. *Phys. A*, **173**, 532 (1991).
[9] A. Jamnik, D. Bratko. Adhesive-hard-sphere model for lyophilic colloidal interaction. *Vestn. Slov. Kem. Drus.*, **38**, 39 (1991).
[10] A. Jamnik. Spatial correlations and solvation interaction in a two-component mixture of adhesive fluids. *J. Chem. Phys.*, **105**, 10511 (1996).
[11] A. Jamnik, D. Bratko. Structure of Baxter adhesive fluid in a planar gap. *Chem. Phys. Lett.*, **203**, 465 (1993).
[12] A. Jamnik, D. Bratko. Structure of confined adhesive fluids—a Monte-Carlo study. *Phys. Rev. E*, **50**, 1151 (1994).
[13] A. Jamnik. Sticky spheres in adhesive pores. *J. Chem. Phys.*, **102**, 5811 (1995).
[14] S. Zhou, A. Jamnik. Analysis of the validity of perturbation density functional theory: based on extensive simulation for simple fluid at spercritical and subcritical temperature under various external potentials. *J. Chem. Phys.*, **122**, 064503 (2005).
[15] S. Zhou, A. Jamnik. Global and critical test of the perturbation density-functional theory based on extensive simulation of Lennard–Jones fluid near an interface and in confined systems. *J. Chem. Phys.*, **123**, 124708 (2005).
[16] S. Zhou. Universal calculational recipe for solvent-mediated potential: based on a combination of integral equation theory and density functional theory. *Chem. Phys. Lett.*, **392**, 110 (2004).
[17] S. Zhou. Universal calculational recipe for the calculation of solvent-mediated potential: (ii) based on density functional theory. *Chem. Phys. Lett.*, **399**, 323 (2004).
[18] S. Zhou. Semi-analytical hard sphere reference system theory for solvent-mediated potential: (III) test and application to system with general interaction potentials. *Chem. Phys. Lett.*, **399**, 315 (2004).
[19] S. Zhou. Isostructural solid–solid transitions in binary asymmetrical hard sphere system: based on solvent-mediated potential. *J. Colloid Interface Sci.*, **288**, 308 (2005).
[20] T.V. Ramakrishnan, M. Yussouff. 1st-principles order-parameter theory of freezing. *Phys. Rev. B*, **19**, 2775 (1979).
[21] D. Henderson. *Fundamentals of Inhomogeneous Fluids*, Marcel Dekker, New York (1992).
[22] G. Rickayzen, A. Augousti. Integral-equations and the pressure at the liquid–solid interface. *Mol. Phys.*, **52**, 1355 (1984).
[23] M. Calleja, A.N. North, J.G. Powels, G. Rickayzen. The structure of fluids confined to spherical pores—theory and simulation. *Mol. Phys.*, **73**, 973 (1991).
[24] S. Zhou, E. Ruckenstein. High order direct correlation functions of uniform fluids and their application to the high order perturbative density functional theory. *Phys. Rev. E*, **61**, 2704 (2000).
[25] S. Zhou. A simple weighted-density functional method: test and its application to hard sphere fluid in spherical cavity. *J. Chem. Phys.*, **110**, 2140 (1999).
[26] S. Zhou. A density functional theory based on universality principle and third order expansion approximation for long-range interaction potential fluids near surfaces. *J. Phys. Chem. B*, **105**, 10360 (2001).
[27] S. Zhou, X. Zhang. High-order perturbative density functional theory for non-uniform long-range interaction potential fluids near surfaces. *J. Colloid Interface Sci.*, **242**, 152 (2001).
[28] S. Zhou. Partitioned density functional approach for Lennard–Jones fluid. *Phys. Rev. E*, **68**, 061201 (2003).
[29] S. Zhou. Mean spherical approximation-based perturbation density functional theory. *Commun. Theor. Phys.* (Beijing, China) **40**, 721 (2003).
[30] S. Zhou. Application of Lagrangian theorem-based density-functional approximation free of adjustable parameters to nonhard-sphere fluid. *J. Chem. Phys.*, **121**, 895 (2004).
[31] P. Tarazona. Free-energy density functional for hard-spheres. *Phys. Rev. A*, **31**, 2672 (1985).
[32] W.A. Curtin, N.W. Ashcroft. Weighted-density-functional theory of inhomogeneous liquids and the freezing transition. *Phys. Rev. A*, **32**, 2909 (1985).
[33] Y. Rosenfeld. Free-energy model for the inhomogeneous hard-sphere fluid mixture and density-functional theory of freezing. *Phys. Rev. Lett.*, **63**, 980 (1989).
[34] S. Zhou, E. Ruckenstein. A density functional theory based on the universality of the free energy density functional. *J. Chem. Phys.*, **112**, 8079 (2000).
[35] M.S. Kim, S.C. Kim. Density functional approximation based on bridge density functionals. *J. Korean Phys. Soc.*, **41**, 343 (2002).
[36] S. Zhou, X. Zhang. Microscopic approach for the site distribution and thermodynamic properties of a single-component polymer subjected to an external field. *Phys. Rev. E*, **64**, 011112 (2001).
[37] S. Zhou, E. Ruckenstein. A new density functional approach to nonuniform Lennard–Jones fluids. *J. Chem. Phys.*, **112**, 5242 (2000).
[38] S. Zhou, X. Zhang. Universality principle and the development of classical density functional theory. *Chin. Phys.*, **11**, 1051 (2002).
[39] S. Zhou, X. Zhang. A new bridge functional and its application to density functional approach for non-uniform fluid. *Acta Phys. Chim. Sinica*, **18**, 699 (2002).
[40] S.C. Kim, S.H. Suh. Inhomogeneous structure of penetrable spheres with bounded interactions. *J. Chem. Phys.*, **117**, 9880 (2002).
[41] S. Zhou. Inhomogeneous mixture system: a density functional formalism based on the universality of the free energy density functional. *J. Chem. Phys.*, **113**, 8719 (2000).
[42] N. Choudhury, S.K. Ghosh. Density functional theory of inhomogeneous fluid mixture based on bridge function. *J. Chem. Phys.*, **114**, 8530 (2001).
[43] S. Zhou. Transformation from Rogers–Young (RY) approximation to density functional approach for non-uniform fluids: numerical recipe. *Phys. Rev. E*, **63**, 051203 (2001).
[44] C.N. Patra, S.K. Ghosh. Structure of nonuniform fluid mixtures: a self-consistent density-functional approach. *J. Chem. Phys.*, **117**, 8933 (2002).
[45] S. Zhou. Formally "exact" first-order Taylor series expansion for density functional theory. *New J. Phys.*, **4**, 36 (2002).
[46] S. Zhou. Functional counterpart of Lagrangian theorem and perturbative density functional theory: a forgotten idea. *Chin. Phys. Lett.*, **19**, 1322 (2002).
[47] S. Zhou. Perturbation density functional theory for density profile of a non-uniform and uniform hard core attractive Yukawa model fluid. *J. Phys. Chem. B*, **106**, 7674 (2002).
[48] S. Zhou. Structure of a confined square-well fluid. *J. Phys. Chem. B*, **107**, 3585 (2003).
[49] S. Zhou. Employing functional counterpart of Lagrangian theorem to improve on density functional theory for density profile of non-uniform fluids. *Chem. Phys.*, **289**, 309 (2003).
[50] S. Zhou. Formally exact truncated nonuniform excess Helmholtz free energy density functional: test and application. *J. Phys. Chem. B*, **108**, 3017 (2004).
[51] S. Zhou. Perturbation density functional theory for nonuniform fluid mixture based on Lagrangian theorem. *Chem. Phys.*, **297**, 171 (2004).
[52] S. Zhou. Further investigation about Lagrangian theorem-based density functional approximation: test by non-uniform polymer melt. *Chem. Phys.*, **310**, 129 (2005).
[53] S. Zhou. Lagrangian theorem-based density functional approach free of adjustable parameter. *Phys. Lett. A*, **319**, 279 (2003).
[54] S. Zhou. Perturbative density functional approximation in the view of weighted density concept and beyond. *Chem. Phys. Lett.*, **385**, 208 (2004).
[55] S. Zhou. A method to incorporate the radial distribution function of bulk fluid into the density functional approximation. *J. Chem. Phys.*, **115**, 2212 (2001).
[56] S. Zhou. Density functional approach based on numerically obtained bridge functional. *Commun. Theor. Phys.* (Beijing, China) **38**, 355 (2002).

[57] Z. Tang, L.E. Scriven, H.T. Davis. Density-functional perturbation theory of inhomogeneous simple fluids. *J. Chem. Phys.*, **95**, 2659 (1991).
[58] A. Kol, B.B. Laird. A partitioned density functional theory of freezing: application to soft spheres. *Mol. Phys.*, **90**, 951 (1997).
[59] M. Quesada-Perez, A. Martin-Molina, R. Hidalgo-Alvarez. Simulation of electric double layers with multivalent counterions: ion size effect. *J. Chem. Phys.*, **121**, 8618 (2004).
[60] N. Choudhury, S.K. Ghosh. New weighted density functional theory based on perturbative approach. *J. Phys. Chem. B*, **107**, 7155 (2003).
[61] S. Zhou. Reformulation of density functional theory for generation of the nonuniform density distribution. *Phys. Rev. E*, **63**, 061206 (2001).
[62] S. Zhou. Specification of density functional approximation by radial distribution function of bulk fluid. *Commun. Theor. Phys.* (Beijing, China) **37**, 543 (2002).
[63] X.C. Zeng, D.W. Oxtoby. Applications of modified weighted density functional theory—freezing of simple liquids. *J. Chem. Phys.*, **93**, 2692 (1990).
[64] D.W. Marr, A.P. Gast. On the solid fluid interface of adhesive spheres. *J. Chem. Phys.*, **99**, 2024 (1993).
[65] S. Zhou. A non-perturbative density functional analysis for non-uniform Lennard–Jones fluid. *J. Chem. Phys.*, **113**, 8717 (2000).
[66] S. Zhou. Extending the simple weighted density approximation for a hard-sphere fluid to a Lennard–Jones fluid: II. Application. *J. Colloid Interface Sci.*, **290**, 364 (2005).
[67] S. Zhou. Extending simple weighted density approximation for hard sphere fluid (I): test. *Int. J. Mod. Phys. B*, **19**, 4701 (2005).
[68] S. Zhou. Density functional approximation for non-hard sphere fluids subjected to external fields. *Int. J. Mod. Phys. B*, **20**, 469 (2006).
[69] D. Frenkel, B. Smit. *Understanding Molecular Simulation*, Academic Press, Boston (1996).
[70] J.J. Potoff, A.Z. Panagiotopoulos. Critical point and phase behavior of the pure fluid and a Lennard–Jones mixture. *J. Chem. Phys.*, **109**, 10914 (1998).
[71] L. Verlet. Integral-equations for classical fluids. 1. The hard-sphere case. *Mol. Phys.*, **41**, 183 (1980).
[72] D.M. Duh, A.D.J. Haymet. Integral-equation theory for uncharged liquids—the Lennard–Jones fluid and the bridge function. *J. Chem. Phys.*, **103**, 2625 (1995).